Real-time analysis of partially polarized light with a space-variant subwavelength dielectric grating

Ze'ev Bomzon, Gabriel Biener, Vladimir Kleiner, and Erez Hasman

Optical Engineering Laboratory, Faculty of Mechanical Engineering, Technion—Israel Institute of Technology, Haifa 32000, Israel

Received September 7, 2001

A novel method for real-time polarization measurement is presented. The method is based on a space-variant wave plate that we realized as a computer-generated space-variant subwavelength dielectric grating. The Stokes parameters of the incident beam are determined by Fourier analysis of the space-variant intensity transmitted through the grating and an analyzer. We discuss the design and realization of such wave plates and demonstrate our technique with polarization measurements of both polarized and partially polarized CO_2-laser radiation at a wavelength of 10.6 μm. © 2002 Optical Society of America

OCIS codes: 260.2130, 260.5430, 050.2770.

Polarization measurements are important for a large range of applications, such as ellipsometry,[1] bioimaging,[2] imaging polarimetry,[3] and optical communications.[4] A commonly used method is to measure the time-dependent signal when a beam is transmitted through a rotating quarter-wave plate (QWP) followed by an analyzer.[5] By Fourier analysis of this signal, one can derive the Stokes parameters of the beam. However, this method requires a sequence of consecutive measurements, making it impractical for real-time polarization measurements in applications such as adaptive polarization-mode dispersion compensation in optical communications. In a previous Letter we presented a method for real-time polarization analysis based on a space-variant (transversely inhomogeneous) polarizer.[6] However, this polarizer made possible the analysis of only fully polarized light.

In this Letter we present a space-domain analogy of the rotating QWP method. Our method is based on a space-varying wave plate, which we realized as a computer-generated space-variant subwavelength dielectric grating. By performing a spatial Fourier analysis of the intensity transmitted through this wave plate, followed by an analyzer, we can measure all four Stokes parameters simultaneously, thus permitting real-time polarization measurement of polarized and partially polarized beams. We discuss the theory behind our method and describe the design and realization processes of our grating. We present experimental measurements of polarized and partially polarized CO_2-laser radiation at a wavelength of 10.6 μm.

Figure 1 is a schematic representation of our concept for real-time polarization measurements. Polarized light from the laser is incident upon a polarization-sensitive medium (e.g., biological tissue, optical fiber, ellipsometric sample, wave plate). The beam is then transmitted through a space-variant wave plate (subwavelength dielectric grating), followed by an analyzer (a subwavelength metal wire grid[7]). The resulting space-variant intensity distribution is imaged onto a camera, and a Fourier analysis of the recorded space-variant intensity is performed, yielding the polarization of the beam that is incident upon the space-varying wave plate, thereby permitting analysis of the sample.

Our approach is conveniently explained by a Stokes representation. In this representation the polarization state is described by a Stokes vector $(S_0, S_1, S_2, S_3)^T$. S_0 is the intensity of the incident beam, and $S_1 \ldots S_3$ represent its polarization state. In general, $S_0^2 \geq S_1^2 + S_2^2 + S_3^2$, with the equality holding for polarized beams.[5] The Mueller matrix that describes the combination of the polarizer and the space-variant wave plate for which the orientation of the fast axis varies linearly in the x direction is

$$M(x) = PR(-ax)WR(ax), \tag{1}$$

where R is the Mueller matrix for a rotator, P is the Mueller matrix for a polarizer, W is the Mueller matrix for a wave plate, and a is the rate of rotation of the fast axis.[5]

Suppose that a monochromatic plane wave in an arbitrary state of polarization, $(S_0, S_1, S_2, S_3)^T$, is incident upon on the apparatus described in Eq. (1). Then, the polarization state of the transmitted beam will be space varying, and its Stokes vector can be found as $[S_0'(x), S_1'(x), S_2'(x), S_3'(x)]^T = M(x)(S_0, S_1, S_2, S_3)^T$. In particular, the transmitted intensity will be

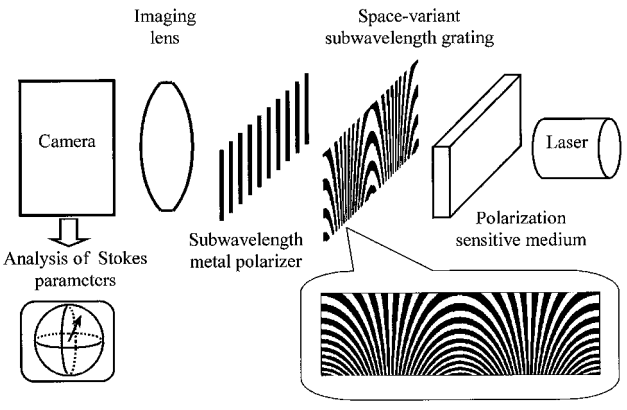

Fig. 1. Schematic presentation of our concept for real-time polarization-state measurements based on a space-varying wave plate and an analyzer. The inset shows the geometry of the subwavelength grating.

0146-9592/02/030188-03$15.00/0

$$S_0'(x) = \frac{1}{4}\Big[AS_0 + \frac{1}{2}(A + C)S_1 + B(S_1 + S_0)\cos 2ax + (BS_2 - DS_3)\sin 2ax + \frac{1}{2}(A - C)(S_1 \cos 4ax + S_2 \sin 4ax)\Big], \quad (2)$$

where $A = {t_x}^2 + {t_y}^2$, $B = {t_x}^2 - {t_y}^2$, $C = 2t_x t_y \cos\varphi$, and $D = 2t_x t_y \sin\varphi$; φ is the retardation of the wave plate, and $t_x t_y$ are its transmission coefficients. Equation (2) describes a truncated Fourier series whose coefficients depend on the Stokes parameters of the incident beam. Therefore, a simple Fourier analysis yields a set of linear equations from which parameters $S_{0,1,2,3}$ can be calculated.

The space-varying wave plate depicted in Fig. 1 can be realized as a space-variant subwavelength dielectric grating. When the period of a grating is smaller than the incident wavelength, only the zeroth order is a propagating order, and the grating behaves as a layer of uniaxial crystal, with the optical axes perpendicular and parallel to the grating grooves.[8] Therefore, by controlling the local period, structure, and direction of the grating, we can create any desired space-variant wave plate. The design and realization of the grating are described below.

First, we define a grating vector $\mathbf{K}_g = K_0(x, y) \times [\cos(ax)\hat{\mathbf{x}} + \sin(ax)\hat{\mathbf{y}}]$, where $\hat{\mathbf{x}}$ and $\hat{\mathbf{y}}$ are unit vectors in the x and y directions, respectively, $K_0 = 2\pi/\Lambda(x, y)$ is the spatial frequency of the grating (Λ is the local period), and ax is the space-variant direction of the vector defined so that it is perpendicular to the grating stripes at each point. To ensure the continuity of the grating, we require that $\mathbf{K}_g$ be a conserving vector, i.e., $\nabla \times \mathbf{K}_g = 0$. This results in a differential equation with the solution $\mathbf{K}_g = (2\pi/\Lambda_0)\exp(ay) \times [\cos(ax)\hat{\mathbf{x}} + \sin(ax)\hat{\mathbf{y}}]$, where Λ_0 is the period at $y = 0$. We can then calculate the grating function ϕ (defined so that $\nabla\phi = \mathbf{K}_g$) by integrating $\mathbf{K}_g$ over an arbitrary path to obtain $\phi(x, y) = (2\pi/a\Lambda_0)\sin(ax)\exp(ay)$. This solution shows that the constraint on the continuity of the grating results in a varying period, which depends on the y coordinate. Therefore, the retardation, φ, and the transmission coefficients, t_x and t_y, of the wave plate also vary in the y direction, as they are period dependent. However, as long as we perform the intensity measurements along lines parallel to the x axis of the grating, the period remains constant and Eq. (2) is valid. We can utilize the varying period of the grating to reduce statistical measurement errors by performing several measurements simultaneously.

We realized a Lee-type binary grating[9] that describes the grating function. The grating was realized as a 5 mm × 3 mm rectangle with $\Lambda_0 = 2\ \mu$m and $a = -18°/\text{mm}$ so that $2\ \mu\text{m} < \Lambda < 5.13\ \mu$m and $-90° < ax < 0°$. First, we fabricated a chrome mask of the grating, using high-resolution laser lithography. The pattern was transferred to a 500-μm-thick GaAs wafer by use of photolithography, after which we etched the grating by electron cyclotron resonance with BCl_3 for 35 min. Finally, we applied an antireflection coating to the back side of the wafer. To examine the fabrication process, we also fabricated a chirped grating whose period varied from 2 to 10 μm by use of the same process.

Figure 2(a) shows scanning electron microscope images of the chirped grating at periods of 2, 3, and 8 μm. We note that the structure of the grating is period dependent, emphasizing the need to determine the dependence of the transmission and the retardation on the local period experimentally. To do this, we illuminated the space-varying grating with light from a CO_2 laser at a wavelength of $\lambda = 10.6\ \mu$m and measured the dependence of the transmission coefficients, t_x and t_y, and the retardation, φ, on the period, using ellipsometric techniques.[5] Figure 2(b) shows the measured transmission coefficients of the grating as well as the theoretical results calculated with rigorous coupled-wave analysis,[10] taking into account the grating profiles shown in Fig. 2(a). There is a good agreement between the calculations and the measurements. The graphs show that when the period is 2–3.24 μm, t_x and t_y do not vary much and have values of approximately 0.95 and 0.82, respectively. At a period of $\lambda/n = 3.24\ \mu$m ($\lambda = 10.6\ \mu$m is the incident wavelength and $n = 3.27$ is the refractive index of GaAs), we notice anomalous behavior that is due to nonzero propagating orders within the GaAs, and the transmission drops sharply. Figure 2(c) shows the measured and the calculated retardation, φ, of the grating at all periods. We notice that φ is close to $\pi/2$ at periods from 2 to 4 μm, after which it begins to vary. Based on these results, we limit our discussion to the areas on the space-varying wave plate where the period is 2–3.24 μm.

Following the measurements, we used the setup depicted in Fig. 1 to test our concept for polarization measurements. We used a CO_2 laser that emitted linearly polarized light at a wavelength of 10.6 μm and replaced the polarization-sensitive medium with a QWP. The images were captured by a Spiricon Pyrocam I, at a rate of 48 Hz. Figure 3(a) shows the measured intensity distributions captured in a single camera frame, at a period of 2.5 μm, as well as the predicted results calculated from Eq. (2), when the

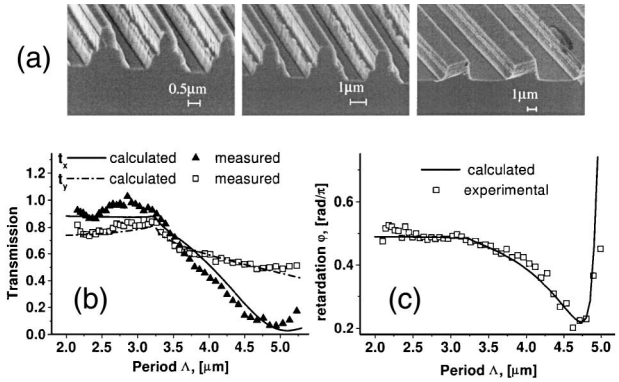

Fig. 2. (a) SEM images of the chirped grating at periods of 2, 3, and 8 μm as well as (b) experimental and calculated dependence of the transmission coefficients, t_x and t_y, and (c) retardation φ on the period.

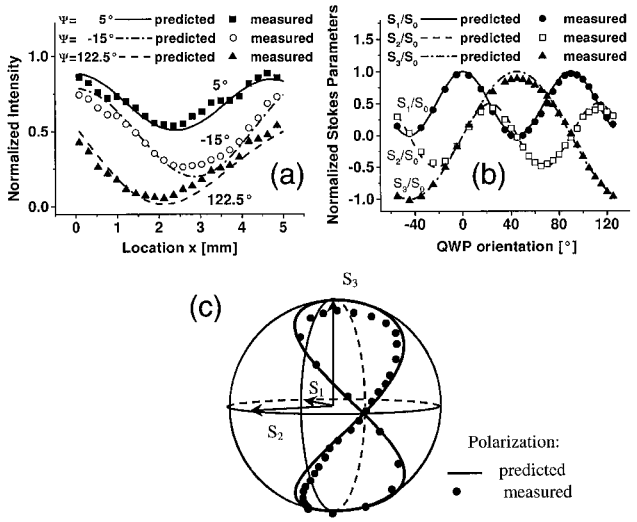

Fig. 3. (a) Normalized transmitted intensity as a function of the x coordinate at a local period of 2.5 μm, when the fast axis of the rotating QWP was at angles of $-15°$, 5°, and 122.5°. (b) Measured and predicted values of the normalized Stokes parameters S_1/S_0, S_2/S_0, and S_3/S_0 as a function of the orientation of the QWP, and (c) these polarization states depicted on the Poincaré sphere.

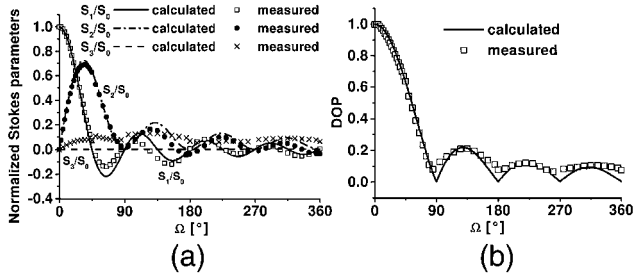

Fig. 4. (a) Measured and predicted values of the normalized Stokes parameters as a function of Ω, as well as (b) measured and predicted DOP.

fast axis of the QWP was at angles of $-15°$, 5°, and 122.5°. The different incident polarizations produce distinct intensity distributions from which their Stokes parameters can be measured. Figure 3(b) shows the measured and predicted Stokes parameters of the resulting beam as a function of the orientation of the QWP. We determined the experimental values by fitting the curve of Eq. (2) to the measured intensity distributions with S_1, S_2, and S_3 as free parameters. The measurements yielded an average error of 1° in the measured azimuthal angle, ψ [$\tan(2\psi) = S_2/S_1$], and an average error of 0.025 in the measured ellipticity, $\tan\chi$ [$\sin(2\chi) = S_3/S_0$]. The standard deviations in the azimuthal angle and ellipticity for a series of successive measurements were 0.7° and 0.5°, respectively. The errors in the polarization measurements result mainly from a small degree of nonuniformity in the structure of the grating caused during fabrication and by fluctuations in the polarization of the light emitted from the laser. The errors can be reduced by improvement of the photolithographic processes and by averaging of the measurements over several periods of the grating. Figure 3(c) depicts the same polarization measurements on the Poincaré sphere. This figure shows all four Stokes parameters simultaneously, thereby emphasizing the good agreement between the predictions and the measurements for polarized light.

Some applications, however, require analysis of partially polarized light. Such beams are characterized by the degree of polarization (DOP), defined as DOP $= \{[\langle S_1(t)\rangle^2 + \langle S_2(t)\rangle^2 + \langle S_3(t)\rangle^2]/\langle S_0(t)\rangle^2\}^{1/2}$, where $\langle\,\rangle$ denotes time-domain averaging. If linearly polarized light is incident upon a half-wave plate (HWP) rotating at frequency ω, then $S_1(t) = \cos(4\omega t)$, $S_2(t) = \sin(4\omega t)$, and $S_3 = 0$. Calculating the DOP yields a value equal to $|(\sin 2\Omega)/2\Omega|$, where Ω is the angle that the HWP was rotated during the time span over which the averaging was performed. We used this calculated value to examine the ability of our method to analyze partial polarization. We chose ω so that the Spiricon Pyrocam captured an image each time the HWP was rotated by 2.5°. We then calculated the average intensity at each pixel on the camera, using all images captured during the rotation of the HWP up to angle Ω, and found the appropriate Stokes parameters. Based on these parameters, we calculated the experimental dependence of the DOP on Ω. Note that the rotating HWP is only a means for simulating partially polarized light and does not play a part in the polarization measurements.

Figure 4(a) shows the measured and predicted Stokes parameters as a function of Ω. We notice that S_3 is close to zero for all values of Ω and that S_1 and S_2 tend to zero as Ω increases. Figure 4(b) shows the measured and predicted DOP. The precision in the measured DOP was 1.6%. We note that as Ω increases the DOP tends to zero, depicting agreement between theory and measurement.

Z. Bomzon's e-mail address is zbomzy@tx.technion.ac.il.

References

1. J. Lee, J. Koh, and R. W. Collins, Opt. Lett. **25,** 1573 (2000).
2. V. Sankaran, M. J. Everett, D. J. Maitland, and J. T. Walsh, Jr., Opt. Lett. **24,** 1044 (1999).
3. G. P. Nordin, J. T. Meier, P. C. Deguzman, and M. W. Jones, J. Opt. Soc. Am. A **16,** 1168 (1999).
4. P. C. Chou, J. M. Fini, and H. A. Haus, IEEE Photon. Technol. Lett. **13,** 568 (2001).
5. E. Collet, *Polarized Light* (Marcel Dekker, New York, 1993).
6. Z. Bomzon, G. Biener, V. Kleiner, and E. Hasman, Opt. Lett. **26,** 1711 (2001).
7. Z. Bomzon, V. Kleiner, and E. Hasman, Opt. Lett. **26,** 33 (2001).
8. S. Y. Chou and W. Dong, Appl. Phys. Lett. **67,** 742 (1995).
9. W. H. Lee, Appl. Opt. **13,** 1677 (1974).
10. M. G. Moharam and T. K. Gaylord, J. Opt. Soc. Am. A **3,** 1786 (1986).